Microchim. Acta 145, 255–260 (2004)
DOI 10.1007/s00604-003-0163-5

Microchimica Acta
Printed in Austria

Original Paper

Microchemical Analysis and Microstructural Development of Cr-Doped Mullites

M. Pilar Villar[1,*], **José M. Geraldía**[2], **Sergio I. Molina**[1,2], and **Rafael García**[1,2]

[1] Universidad de Cádiz, Dpto. Ciencia de los Materiales e Ingeniería Metalúrgica y Química Inorgánica, Campus Río San Pedro, P.O. Box 40, E-11510 Puerto Real (Cádiz), Spain
[2] Universidad de Cádiz, SCCYT, División de Microscopía Electrónica, Campus Río San Pedro, E-11510 Puerto Real (Cádiz), Spain

Received May 22, 2003; accepted October 20, 2003; published online February 27, 2004

Abstract. A characterization study of chromium doped sol–gel mullites (with Cr_2O_3 contents varying between 1 and 9 wt.%) by means of electron beam techniques is presented. Scanning and transmission electron microscopy studies gave information about general microstructural features, like grain size and shape, presence of glassy phase in triple grain junctions and segregation of secondary crystalline phases. EDX-TEM measurements reveal an upper solubility of chromium in the mullite lattice of approx. 8 wt.% Cr_2O_3. The effect of Cr doping in the microstructural development of these mullites is discussed.

Key words: Chromium; mullite; aluminosilicate; microstructural development; transition metal doping.

Mullite is the only stable phase formed in the Al_2O_3–SiO_2 system at atmospheric pressure, with the general formula $Al_2[Al_{2+2x}Si_{2-2x}]O_{10-x}$, being x the number of oxygen vacancies per unit cell, $0.17 \leq x \leq 0.59$. Its lattice can be described by an orthorhombic cell consisting of chains of edge-sharing AlO_6 octahedra running along the c axis, and cross-linked by $(Si,Al)O_4$ tetrahedral double chains [1, 2]. Mullite is very much appreciated as an advanced ceramic because of its good high-temperature mechanical properties and low thermal conductivity and expansion [1–3]. Modifications on the synthesis methods or compositions of mullite have been studied in order to further improve some of these properties [4, 5]. Doping of mullite with chromium induces a decrease in its thermal expansion coefficient [6, 7], making this material suitable for silicon-on-ceramics applications.

The main objective of the present work is the characterization of the microstructural evolution of chromium doped sol–gel mullites by means of electron beam techniques, as well as determining the maximum amount of this transition metal admissible in these aluminosilicate systems. The full comprehension of the microstructure of these ceramics could help to understand some aspects of their behavior.

Experimental

Five different compositions of alcoxide-derived (TEOS, aluminum sec-butylate and chromium acetate) sol–gel mullites were studied (stoichiometric -non-doped- 3:2 mullite, and 1, 3, 6 and 9 wt.% Cr_2O_3 doped mullites), each one being sintered at two different temperatures (1650 and 1750 °C). Samples will be named M0, M1, M3, M6 and M9 (depending of the Cr-content) followed by "–" plus the sintering temperature (e.g. M0-1650 for non-doped mullite sintered at 1650 °C).

* Author for correspondence. E-mail: pilar.villar@uca.es

SEM studies were performed on polished, thermally etched and Au- or C-coated samples using a Jeol JSM 820 electron microscope. Grain size and shape were measured using the image analysis program Global Lab Image 3.1 (Data Translation, Inc. & Acuity Imaging, Inc.). TEM and HREM observations were carried out using two electron microscopes, Jeol 1200EX TEM/STEM and Jeol 2000EX, respectively, after dimple grinding, Ar^+ ion milling, and carbon coating of 3 mm discs of the ceramics. Compositional profiles were obtained by EDX on TEM mode with an EDX analyzer model Link AN/10000 attached to the Jeol 1200EX TEM/STEM electron microscope. Glassy phase distribution was studied with a diffuse dark field technique.

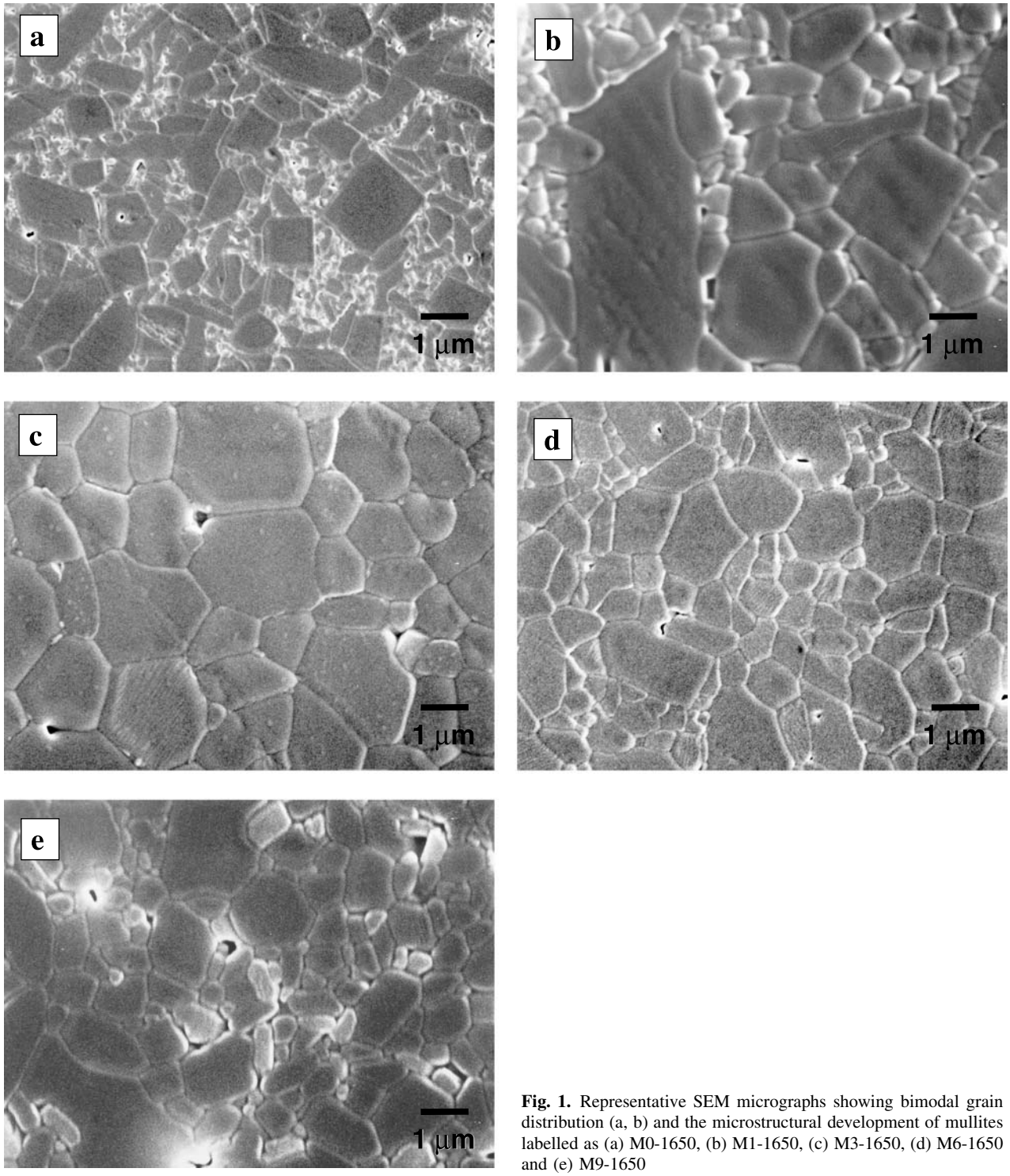

Fig. 1. Representative SEM micrographs showing bimodal grain distribution (a, b) and the microstructural development of mullites labelled as (a) M0-1650, (b) M1-1650, (c) M3-1650, (d) M6-1650 and (e) M9-1650

Results and Discussion

SEM studies were performed to describe the microstructural development of the different mullites, considering the variation of their main features (grain size and shape, existence of other crystalline phases, etc.) versus dopant content and sintering temperature. Figures 1 (showing bimodal grain distribution for non-doped and lowest Cr-content mullites) and 2 contain illustrative SEM micrographs of the studied samples. Increasing sintering temperature always implies

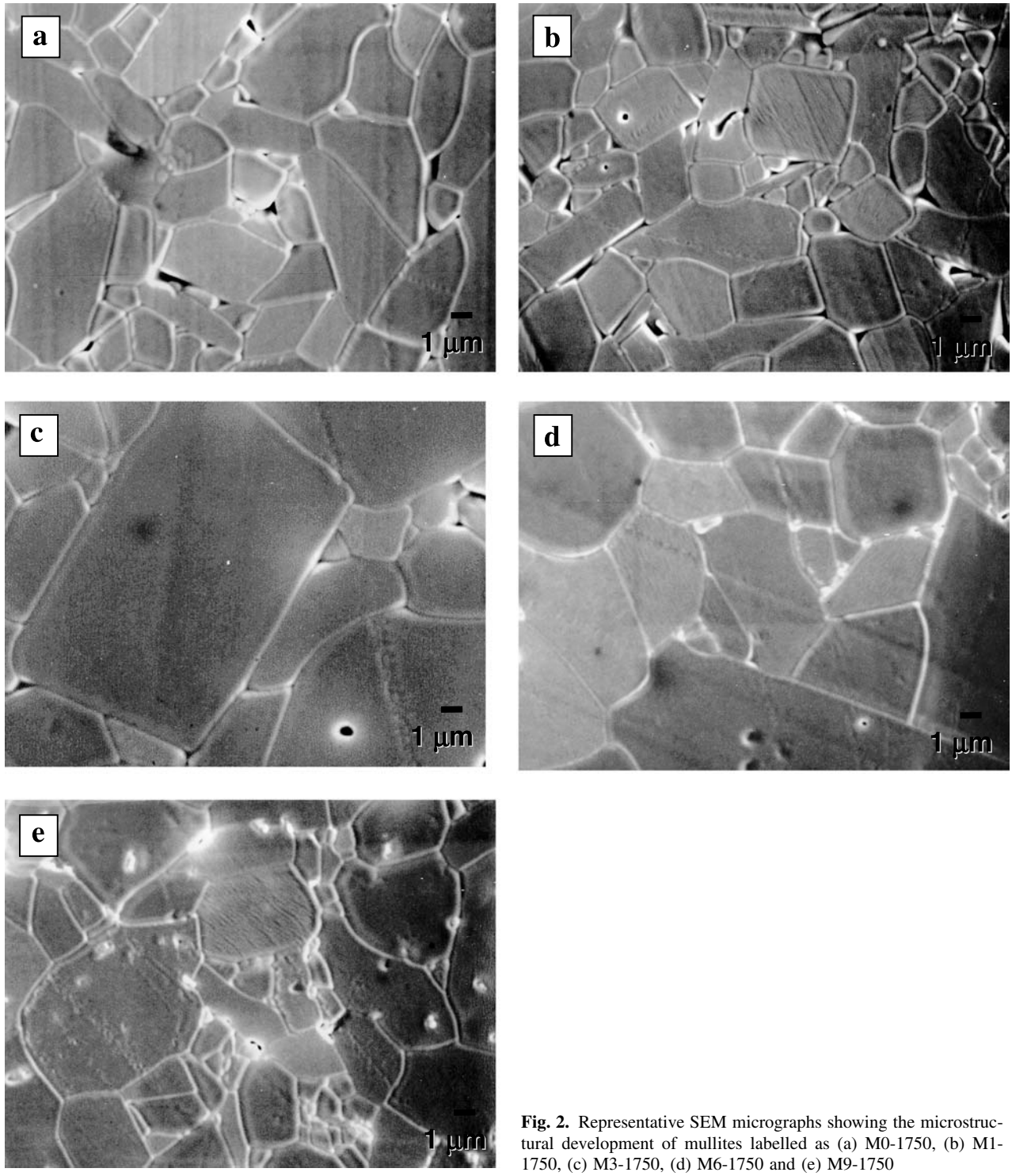

Fig. 2. Representative SEM micrographs showing the microstructural development of mullites labelled as (a) M0-1750, (b) M1-1750, (c) M3-1750, (d) M6-1750 and (e) M9-1750

larger grain sizes and more heterogeneous grain shapes considering the same compositions, while the Cr content in the samples promotes a progressive polygonization of the crystals. This last effect is more evident in the M3-1650 mullite. Grain sizes measurements also reveal maximum sizes for the M3 samples. Data are collected in Table 1. Polygonization of grains with significant contents of dopant (3 wt.% Cr_2O_3, at least) indicates that this transition metal induces similar effects in grain growth as those produced by an Al-enrichment of mullites, as it has been reported previously [8]. This fact has been related to different nucleation and grain growth mechanisms depending on the bulk composition of these aluminosilicate systems. The similarity of grain growth behavior in

Table 1. Grain sizes measurements for mullite in samples sintered at 1650 and 1750 °C (confidence interval at 95% of the average)

Material	Grain size (nm)	Material	Grain size (nm)
M0-1650	477.64 ± 15.06	M0-1750	485.68 ± 15.14
M1-1650	403.35 ± 15.28	M1-1750	450.20 ± 18.39
M3-1650	1392.9 ± 77.82	M3-1750	2331.4 ± 321.1
M6-1650	521.43 ± 23.81	M6-1750	861.92 ± 210.28
M9-1650	625.56 ± 38.24	M9-1750	772.52 ± 77.26

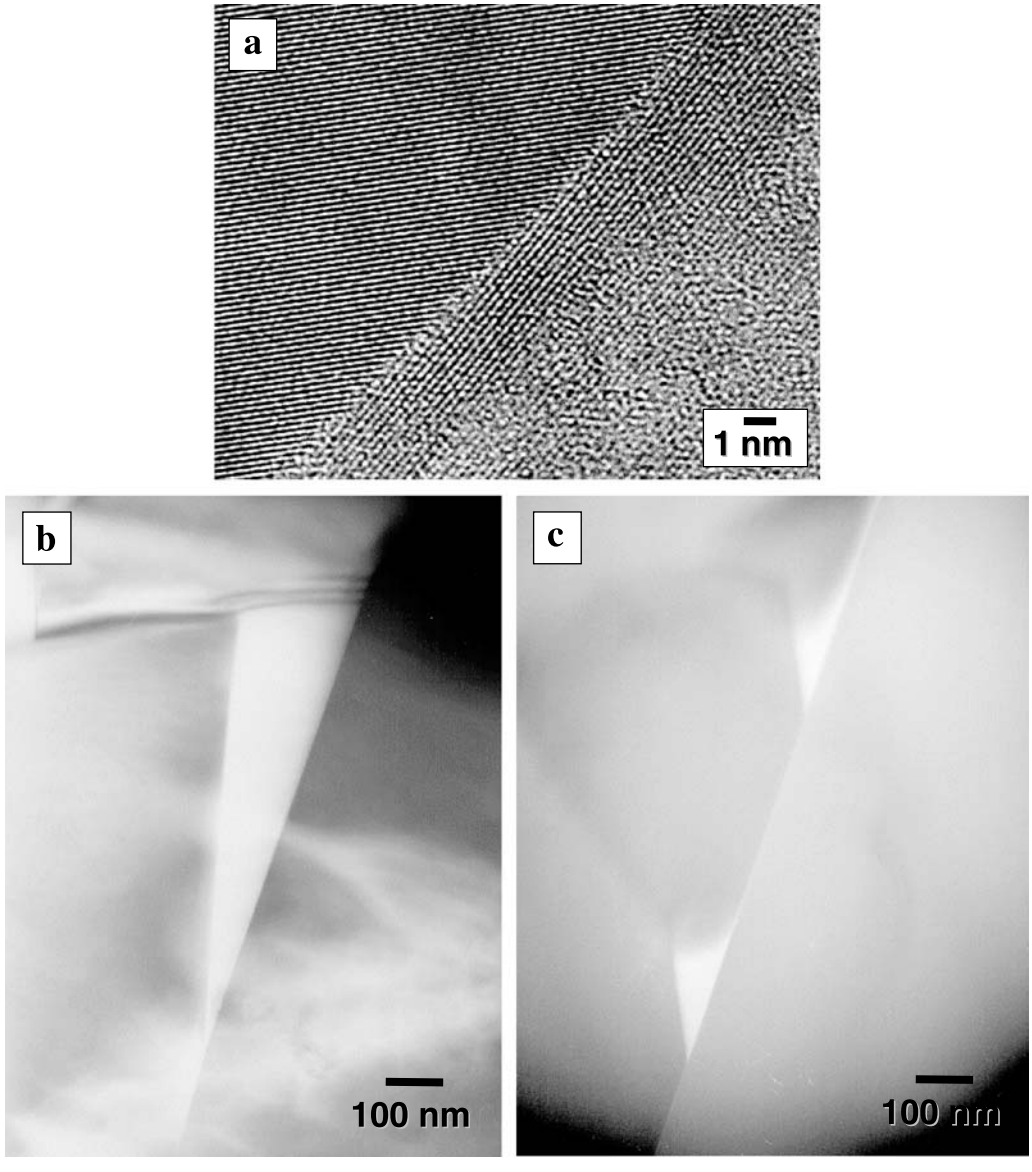

Fig. 3. (a) HREM micrograph of a typical grain boundary free of glassy phase in sample M3-1650. Examples of glass in triple grain junctions for (b) M1-1750 and (c) M6-1750

Table 2. EDX measurements (wt.% of the corresponding oxide) for each phase (confidence interval at 95% of the average)

	Mullite			Glass			$(Al,Cr)_2O_3$		
	Al_2O_3	SiO_2	Cr_2O_3	Al_2O_3	SiO_2	Cr_2O_3	Al_2O_3	SiO_2	Cr_2O_3
M0-1650	n.m.	n.m.	n.m.	n.m.	n.m.	n.m.	n.m.	n.m.	n.m.
M0-1750	72.9 ± 0.3	27.1 ± 0.3	–	13.1 ± 3.2	86.9 ± 3.2	–	–	–	–
M1-1650	73.6 ± 0.3	25.9 ± 0.2	0.5 ± 0.0	–	–	–	–	–	–
M1-1750	n.m.	n.m.	n.m.	n.m.	n.m.	n.m.	n.m.	n.m.	n.m.
M3-1650	71.6 ± 0.3	24.8 ± 0.3	3.6 ± 0.1	–	–	–	–	–	–
M3-1750	71.0 ± 1.2	25.4 ± 1.5	3.6 ± 0.4	–	–	–	–	–	–
M6-1650	69.1 ± 0.6	25.2 ± 0.7	5.7 ± 0.2	–	–	–	–	–	–
M6-1750	69.2 ± 0.2	25.4 ± 0.2	5.4 ± 0.1	18.5 ± 2.0	80.4 ± 2.4	1.1 ± 0.6	–	–	–
M9-1650	68.1 ± 0.7	25.4 ± 1.0	6.5 ± 0.4	–	–	–	77.0 ± 0.4	0.6 ± 0.3	22.4 ± 0.6
M9-1750	67.9 ± 1.1	24.5 ± 0.8	7.6 ± 0.4	–	–	–	73.7 ± 0.4	0.8 ± 0.4	25.5 ± 0.4

n.m. Not measured.

Cr-doped mullites and Al-rich mullites can be considered as additional proof for the idea of substitution of Al^{3+} by Cr^{3+} in the mullite lattice as suggested by other authors [9].

Glassy phase in triple grain junctions and grain boundaries is also less abundant when the chromium content increases, although it is more evident in samples sintered at higher temperature (Fig. 3), as expected. Another consequence of the Al^{3+} replacement described above is its reaction with the remaining amorphous material to produce more crystals or stimulate the growth of the existing ones. This would justify the decrease of glass contents with increasing Cr additions.

On the other hand, backscattered electron SEM showed two significant effects: a lower porosity level in mullites sintered at 1750 °C and the segregation of a second phase in the 9 wt.% Cr_2O_3 doped mullites. This second phase was found homogeneously distributed in both samples (sintered at 1650 and 1750 °C), and was identified as a member of the Al_2O_3–Cr_2O_3 solid solution. Volatility of Cr and its difficult sinterability has been previously reported for Cr_2O_3-doped yttria-stabilized zirconia [10], and the same effect would be the responsible of porosity in mullites sintered at 1650 °C, although this could be compensated by a better sinterability at higher temperatures (1750 °C) due to the higher content of remaining and agglutinative glassy phase.

Microchemical analysis was performed on the most of electron-transparent samples by means of TEM-EDX, obtaining the composition of the different phases present: mullite or Cr-doped mullite, glass and $(Al,Cr)_2O_3$ phase. The results of these analyses are summarized in Table 2 and clearly indicate an upper limit of dopant cation in the mullite lattice of ~8 wt.%, being this incorporation higher in the 1750 °C sintered material. The rest of the dopant reacts with Al_2O_3 to segregate as the second phase indicated above. This fact is in accordance with the predictions of the phase diagram for the ternary Al_2O_3–Cr_2O_3–SiO_2 system. The degree of Cr incorporation seems to be related with the synthesis method, since the presence of this $(Al,Cr)_2O_3$ phase has not been reported in Cr-doped aluminosilicates obtained by conventional powder reaction methods [11, 12].

Conclusions

A general microstructural and microchemical characterization of sol–gel Cr-doped mullites was performed. A limit of Cr content in the mullite lattice was found at approx. 8 wt.% Cr_2O_3. Higher chromium additions promote the segregation of a second crystalline phase $(Al,Cr)_2O_3$ in the system. The composition of this phase was determined in our systems. On the other hand, chromium induces a certain polygonization of the mullite grains, mostly in the M3 samples. At the same time, this composition results in the largest grain sizes. Glass contents are inhibited by the Cr doping, although they increase with sintering temperatures. Substitution of Al^{3+} by Cr^{3+} in the mullite lattice is connected with these features.

Acknowledgements. Authors are gratefully indebted to Dr. Schneider and Dr. Saruhan (DLR, Cologne, Germany), for providing the mullites examined in this work. All the electron microscope studies have been performed in the facilities of the University of Cádiz (SCCYT, División de Microscopía Electrónica). M.P.V. also thanks to Dr. Rojas and Dr. Fernández-Camacho (Instituto de Ciencia de Materiales de Sevilla, Spain) for allowing the use of the grain size and shape measurement software.

References

[1] Somiya S, Davis R F, Pask J A (eds) (1990) Ceramics transactions, vol. 6, mullite and mullite matrix composites. American Ceramic Society. Westerville, OH
[2] Schneider H, Okada K, Pask J A (eds) (1994) Mullite and mullite ceramics. John Wiley & Sons, Chichester
[3] Torrecillas R, Calderón J M, Moya J S, Reece M J, Davies D K L, Olagnon C, Fantozzi G (1999) J Eur Ceram Soc 19: 2519–2527
[4] Okada K, Otsuka N, Somiya S (1991) Bull Am Ceram Soc 70: 1633–1640
[5] Fonseca A M L M, Ferreira J M F, Salvado I M M, Baptista J L (1997) J Sol–Gel Sci Technol 8: 403–407
[6] Villar M P, Geraldía J M, Gago-Duport L (1994) Mat Res Soc Symp Proc 136: 757–762
c [7] Villar M P (2000) Cristalización y desarrollo microestructural de mullitas sol–gel dopadas con cromo. PhD Thesis, University of Cádiz
[8] Saruhan B, Voß U, Schneider H (1994) J Mater Sci 29: 3261–3268
[9] Rager H, Schneider H, Graetsch H (1990) Amer Mineral 75: 392–397
[10] Hirano S, Yoshinaka M, Hirota K, Yamaguchi O (1996) J Am Ceram Soc 79: 171–176
[11] Bauchspieß K R, Schneider H, Kulikov A (1996) J Eur Ceram Soc 16: 203–209
[12] Piriou B, Rager H, Schneider H (1996) J Eur Ceram Soc 16: 195–201